PACS numbres: 65.80.Ck, 72.15.Jf, 72.20.Pa, 72.80.Vp, 81.05.ue
DOI: 10.3367/UFNr.0182.201211j.1229

Anomalous thermoelectric and thermomagnetic properties of graphene

A A Varlamov, A V Kavokin,
I A Luk'yanchuk, S G Sharapov

1. Introduction

We present the results of recent investigations of some anomalies of thermoelectric and thermomagnetic properties of graphene. In Section 3, we show that the presence of a gap in the Dirac spectrum (the possibility of its existence under certain conditions is actively discussed in the literature) leads to the appearance of a characteristic peak in the thermopower as the chemical potential approaches the gap edge. The height of this peak can exceed the magnitude of the graphene thermopower, which is large by itself, by an order of magnitude. The giant effect revealed is related to the appearance, with the chemical potential approaching the edge of the gap, of a new channel of scattering of quasiparticles by impurities, with the relaxation time that essentially depends on energy. The analysis of this feature, which is based on the Kubo formalism, reproduces the well-known results for gapless graphene, but demonstrates the inapplicability of the simple Mott formula in the case under consideration.

In Section 4, we discuss the specific behavior of quantum oscillations of the Nernst coefficient (NC) that are observed in graphene and graphite upon the application of sufficiently strong magnetic fields. We shown how the character of the spectrum of quasiparticles of a sample can be judged from the character of these oscillations.

2. On the history of thermoelectricity

The control of heat fluxes and the minimization of related losses are important factors in designing modern elements of nanoelectronics, including those based on the application of graphene [1]. Experiments [2] show that the thermoelectric effect can lead to a significant change in temperature (up to 30%) in the region of contacts and can therefore play a substantial role in the problem of cooling contacts. The experimentally measured magnitude of the graphene thermopower at room temperature can reach $k_B/e \sim 100$ μV K^{-1} (here, k_B is the Boltzmann constant and $-e < 0$ is the electron charge).

The study of thermoelectric and thermomagnetic phenomena has a two-century history. The thermoelectric effect, consisting in the appearance of electric current in a circuit that includes two different metals whose contacts are maintained at different temperatures, was discovered in 1821 by an Estonian–German scientist, Thomas Johann Seebeck. Quantitatively, the Seebeck effect is characterized by the differential thermopower (Seebeck coefficient, i.e., the thermoelectromotive force arising in an inhomogeneously heated conductor) divided by the corresponding temperature difference:

$$S_{xx} = -\lim_{\Delta T\to 0}\frac{\Delta V}{\Delta T} = \frac{E_x}{\nabla_x T}\,.$$

The thermopower of metals is usually small (about 10^{-8} V K^{-1}), but can be much greater in doped semiconductors and in semimetals.

More than a century later [3], an English scientist, Neville Mott, found an important relationship between the differential thermopower and the logarithmic derivative of the longitudinal electric conductivity $\sigma_{xx}(\mu, T)$ of a metal:

$$S_{xx}(\mu, T) = -\frac{\pi^2}{3e}\,k_B T\,\frac{\mathrm{d}}{\mathrm{d}\mu}\left[\ln\sigma_{xx}(\mu, T=0)\right], \qquad (1)$$

where μ is the chemical potential of charge carriers and T is the temperature. At present, this formula is basic in analyzing experiments related to thermoelectricity; however, numerous anomalous situations are known where the behavior of the thermopower cannot be described by the Mott formula. These are phenomena such as an increase in the thermopower of metals at temperatures close to the Kondo temperature and the anomalies of thermopower at electron topological transitions and its oscillations in strong magnetic fields. One of the factors responsible for the invalidity of the Mott formula is the existence (due to one reason or another) of an essential dependence of the relaxation time of charge carriers on the energy.

Among the variety of known thermomagnetic phenomena, those discussed most frequently are the effects of Nernst and Nernst–Ettingshausen, discovered by Austrian scientists Albert von Ettingshausen and Walter Nernst in 1886. The Nernst effect in metals [4], which is a thermal analog of the Hall effect, consists in the appearance of an electric field E_y perpendicular to the mutually perpendicular magnetic field H ($\|z$) and temperature gradient $\nabla_x T$. In this case, it is assumed that all electrical circuits are open, i.e., $J_x = J_y = 0$, and no heat flux is present along the y axis (the adiabaticity condition). Quantitatively, the effect is characterized by the NC:

$$\nu = \frac{E_y}{(-\nabla_x T)\,H}\,.$$

The NC can change, depending on the material, within several orders of magnitude, from 7 μV K^{-1} T^{-1} in bismuth to 10^{-5} mB K^{-1} T^{-1} in "good" metals [5].

The Nernst–Ettingshausen effect is a different experimental realization of the Nernst effect: the electrical current is passed along the y axis through a sample placed into a magnetic field directed along the z axis; along the x axis, a

A A Varlamov National University of Science and Technology MISiS, Moscow, Russian Federation;
University of Rome "Tor Fergata," Rome, Italy
E-mail: varlamov@ing.uniroma2.it
A V Kavokin Landau Institute of Theoretical Physics, RAS, Moscow, Russian Federation;
University of Southhampton, UK; St. Petersburg State University, St. Petersburg, Russian Federation
I A Luk'yanchuk Landau Institute of Theoretical Physics, RAS, Moscow, Russian Federation;
University of Picardie Jules Verne, France
S G Sharapov Bogolyubov Institute of Theoretical Physics, National Academy of Sciences of Ukraine, Ukraine

Uspekhi Fizicheskikh Nauk **182** (11) 1229 – 1234 (2012)
DOI: 10.3367/UFNr.0182.201211j.12293
Translated by S N Gorin; edited A M Semikhatov

temperature gradient arises in this case. Below, we do not distinguish between these effects.

The microscopic nature of the Nernst effect remained unclear up to 1948, until Sondheimer [6], using a kinetic equation, found an expression for the NC of a degenerate electron gas with impurities, by relating the NC to the derivative of the Hall angle $\theta_{\rm H} = \sigma_{xy}/\sigma_{xx}$ with respect to energy:

$$v(T) = -\frac{\pi^2}{3}\frac{cT}{eH_z}\frac{\partial}{\partial\mu}\left(\frac{\sigma_{xy}}{\sigma_{xx}}\right) = -\frac{\pi^2 T}{3m}\frac{{\rm d}\tau(\varepsilon)}{{\rm d}\varepsilon}\bigg|_{\varepsilon=\mu}, \qquad (2)$$

which permitted him to find the relation between these two effects and made the Nernst effect an important tool for studies of the character of scattering of charge carriers in semiconductors. In (2), m is the effective mass of charge carriers and $\tau(\varepsilon)$ is the energy-dependent relaxation time.

Within the Sondheimer theory, the coefficient v is constant in weak fields and decreases as H^{-2} in sufficiently strong fields, when the cyclotron frequency $\omega_{\rm c}$ exceeds τ^{-1} (the reciprocal value of the relaxation time). In 1964, Obraztsov [7] noted the importance of taking so-called magnetization currents (electric currents arising because of the inhomogeneous magnetization of a sample) into account in discussing the Nernst effect.

In Sections 3 and 4, we present the results of two recent investigations [8, 9] of unusual thermoelectric and thermomagnetic effects in a "hot" field in the physics of condensed state, the study of properties of graphene and related systems.

3. Thermoelectric effect in graphene with a gap in its spectrum

The results of experiments [10–13] on the measurements of thermoelectric transport in graphene can mainly be explained theoretically using the Mott formula. Nevertheless, these experiments showed that Mott formula (1) gives results that do not correspond to experimental data when, at high temperatures, μ is close to the Dirac point, especially in graphene samples with a high mobility [13]. The theoretical analysis in [14–16] shows that this discrepancy is related to the violation of the conditions for the applicability of the Mott formula, which have the form $T \ll |\mu|$ and/or $T \ll \zeta$ (where ζ is the characteristic energy scale at which a change occurs in the conductivity $\sigma_{xx}(\mu, T = 0)$ near the Fermi surface).

Below, we show that the thermopower in graphene, which is already high, may be increased additionally by about an order of magnitude due to the opening of a gap Δ in the spectrum of quasiparticle excitations. This leads to the appearance of a new channel of scattering of quasiparticles, and because the relaxation time depends strongly on energy, this leads to the appearance of a giant peak in the thermopower when the chemical potential approaches the edge of the gap. This picture is very similar to the well-known thermopower anomaly near the electron topological transition (see review [17]).

We note that experiments [18, 19] indicate the presence of a gap in the spectrum of quasiparticle excitations in graphene near the Dirac point, which seems to be related to the effect of the substrate. For single-layer graphene, the problem of the existence of a gap has been studied insufficiently. Our results allow suggesting measurements of thermopower as a sensitive method for revealing a gap.

3.1 Electron scattering in gapped graphene

In the momentum representation, the Hamiltonian of graphene is written as

$$\widehat{H} = \sum_{\sigma}\int_{\rm BZ}\frac{{\rm d}^2 p}{(2\pi)^2}\,\Upsilon_\sigma^\dagger(\mathbf{p})\left[\widehat{\mathcal{H}}(\mathbf{p}) - \mu\,\widehat{\tau}_0\right]\Upsilon_\sigma(\mathbf{p})\,, \qquad (3)$$

where

$$\widehat{\mathcal{H}}(\mathbf{p}) = \widehat{\tau}_+\phi(\mathbf{p}) + \widehat{\tau}_-\phi^*(\mathbf{p}) + \Delta\,\widehat{\tau}_3\,,$$

$\widehat{\tau}_0$, $\widehat{\tau}_3$, and $\widehat{\tau}_\pm = (\widehat{\tau}_1 \pm {\rm i}\,\widehat{\tau}_2)/2$ are the Pauli matrices acting in the space of sublattices on the spinors $\Upsilon_\sigma(\mathbf{p})$ and $\Upsilon_\sigma^\dagger(\mathbf{p}) = \left(a_\sigma^\dagger(\mathbf{p}),\, b_\sigma^\dagger(\mathbf{p})\right)$ with the electron creation (annihilation) operators $a_\sigma^\dagger(\mathbf{p})$, $b_\sigma^\dagger(\mathbf{p})$ $\left(a_\sigma(\mathbf{p}),\, b_\sigma(\mathbf{p})\right)$, which correspond to the sublattices of components A and B; σ is the spin index; and the integration is performed over the Brillouin zone (BZ). In the case under consideration, the complex function $\phi(\mathbf{p})$ responsible for the dispersion can be chosen near two independent K points of the BZ in the form $\xi \equiv |\phi(\mathbf{p})| = \hbar v_{\rm F}|\mathbf{p}|$, where $v_{\rm F}$ is the Fermi velocity, and the wave vector $\mathbf{p}$ is referenced to the corresponding K point. The presence of the gap Δ violates the equivalence of the A and B sublattices, and the spectrum near the K points takes the form $E(\mathbf{p}) = \pm(\hbar^2 v_{\rm F}^2\mathbf{p}^2 + \Delta^2)^{1/2} - \mu$.

Scattering by impurities is considered using the Abrikosov–Gor'kov technique in terms of the self-consistent Born approximation. The scattering potential is chosen such that the scattering between different valleys could be neglected; within a single valley, the potential is assumed to be constant, equal to $u(\mathbf{0})$. As a result, we obtain the following expression for the scattering by impurities:

$$\Gamma(\varepsilon) = \Gamma_0\left(\frac{|\varepsilon+\mu|}{|\mu|} + \frac{\Delta^2}{|\varepsilon+\mu||\mu|}\right)\theta\left((\varepsilon+\mu)^2 - \Delta^2\right), \qquad (4)$$

where $\Gamma_0 = 2\hbar/\tau_0$, τ_0 is the characteristic relaxation time, $\tau_0^{-1} = n_i|u(\mathbf{0})|^2|\mu|/(4\hbar^3 v_{\rm F}^2)$ [20], n_i is the concentration of charge carriers, and θ is the Heaviside function. In the results presented below, we use the value $\Gamma_0 = 20$ K, neglecting the concentration dependence. It follows from Eqn (4) that the scattering is absent at $(\varepsilon+\mu)^2 < \Delta^2$. Nevertheless, we note that some processes that have not been taken into account in the model lead to a finite relaxation time below the edge of the gap. In numerical calculations, this is taken into account by adding a small residual scattering γ_0 to $\Gamma(\varepsilon)$. The final results are almost independent of the magnitude of γ_0.

3.2 Thermopower in gapped graphene

Using the Kubo formula, the following expressions can be obtained for the electrical conductivity and thermoelectric coefficient:

$$\left\{\begin{matrix}\sigma_{xx}\\ \beta_{xx}\end{matrix}\right\} = \frac{e^2}{\hbar}\int_{-\infty}^{\infty}\frac{{\rm d}\varepsilon\,\mathcal{A}(\varepsilon,\Gamma(\varepsilon),\Delta)}{2T\cosh^2\left[\varepsilon/(2T)\right]}\left\{\begin{matrix}1\\ \dfrac{\varepsilon}{eT}\end{matrix}\right\}, \qquad (5)$$

where at a nonzero gap Δ, the function $\mathcal{A}$ has the form [21, 22]

$$\mathcal{A}(\varepsilon,\Gamma(\varepsilon),\Delta) = \frac{1}{2\pi^2}\left[1 + \frac{(\mu+\varepsilon)^2 - \Delta^2 + \Gamma^2(\varepsilon)}{2|\mu+\varepsilon|\,\Gamma(\varepsilon)}\right.$$
$$\left.\times\left(\frac{\pi}{2} - \arctan\frac{\Delta^2 + \Gamma^2(\varepsilon) - (\mu+\varepsilon)^2}{2|\mu+\varepsilon|\,\Gamma(\varepsilon)}\right)\right]. \qquad (6)$$

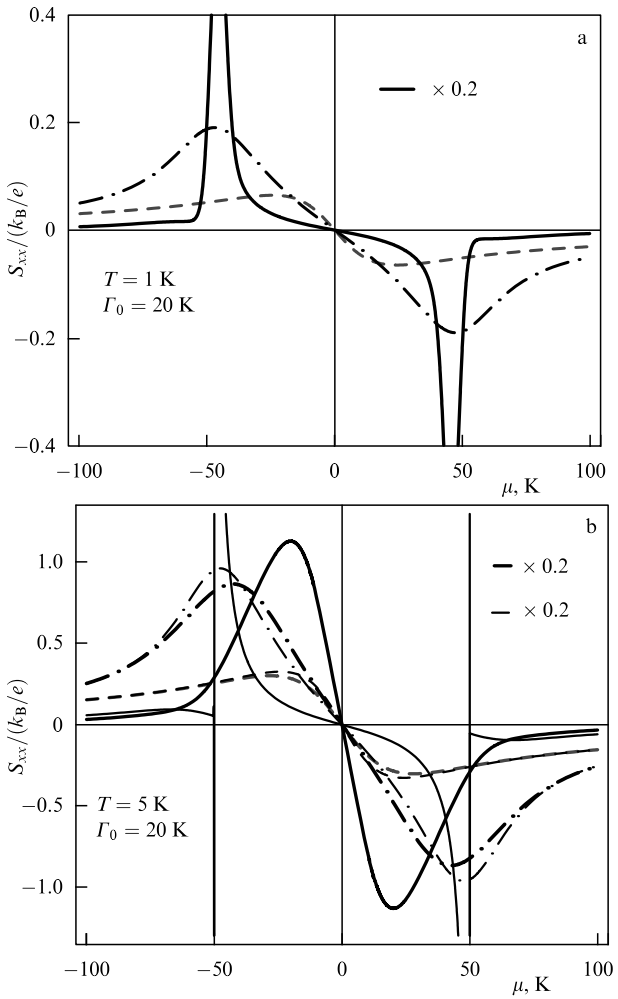

Figure 1. (Available in color online.) Thermopower S_{xx} (in k_B/e units) as a function of the chemical potential μ at (a) $T = 1$ K and (b) $T = 5$ K. The dashed curves correspond to the energy-independent $\Gamma = \Gamma_0$ and $\Delta = 0$; dashed-dotted thick curves to $\Gamma = \Gamma_0$ and $\Delta = 50$ K; solid thick curves to the energy-dependent $\Gamma(\varepsilon)$ and $\Delta = 50$ K. The dependences shown by continuous lines have been multiplied by 0.2. The thin curves in (b) have been obtained via the Mott formula.

At $\Delta = 0$, Eqn (6) is simplified to the form considered in [14, 16]. In this case, assuming that $\Gamma(\varepsilon) = \Gamma_0 = \text{const}$ and that $|\mu| \gg T$, Γ_0, we find that $\sigma_{xx} = e^2|\mu|/(2\pi\hbar\Gamma_0)$ and $\beta_{xx} = \pi e T \operatorname{sgn}\mu/(6\hbar\Gamma_0)$, in accordance with the results in [22]. Then the thermopower $S_{xx} = -\beta_{xx}/\sigma_{xx}$ is the same as in usual metals, $S_{xx} = -(\pi^2/3e)\,T/\mu$, and coincides with the value that directly follows from Mott formula (1).

The $S_{xx}(\mu)$ dependences at $T = 1$ K and $T = 5$ K are shown in Fig. 1. The thick dashed curves correspond to the case $\Delta = 0$, $\Gamma(\varepsilon) = \Gamma_0$, with $\sigma_{xx}(\mu) \propto |\mu|$ and $S_{xx}(\mu) \propto 1/\mu$ at large $|\mu|$. Expressions (5) and (6) also allow reproducing the results in the case of a nonzero gap and an energy-independent $\Gamma(\varepsilon) = \Gamma_0$ [21, 22]. The corresponding dependences are shown by thick dashed-dotted curves, calculated at $\Delta = 50$ K.

Our main result, shown by thick solid curves, was obtained for the energy-dependent $\Gamma(\varepsilon)$ given by Eqn (4), at $\Delta = 50$ K. We note that the corresponding values of $S_{xx}(\mu)$ were diminished fivefold to show them together with the other curves in the figure. This means that the peak values of the thermopower are at least fivefold greater than the magnitude of the thermopower obtained for $\Gamma(\varepsilon) = \text{const}$.

A substantial increase in the thermopower in the case of the energy-dependent $\Gamma(\varepsilon)$ can already be expected even on the basis of the Mott formula (1). Nevertheless, formula (1) cannot be used for a quantitative description. Indeed, the thin curves in Fig. 1b were obtained with the use of data for the electrical conductivity at the zero temperature $\sigma(\mu, T = 0) = (2e^2/\hbar)\,\mathcal{A}(0, \Gamma(0), \Delta)$ and Mott formula (1), whereas the thick curves were derived using the Kubo formula for both σ_{xx} and β_{xx}. It is seen that the agreement between the Kubo and Mott formulas is quite good for $\Delta = 0$ and $\Gamma(\varepsilon) = \text{const}$, and becomes ideal at $T = 1$ K; therefore, the results for the Mott formula are not given in Fig. 1a. At the same time, it can be seen from Fig. 1b that for a finite value of Δ and $\Gamma(\varepsilon) = \text{const}$, a discrepancy is already observed between the results obtained using the Kubo and Mott formulas, especially near $|\mu| = \Delta$. Finally, in the case of an energy-dependent $\Gamma(\varepsilon)$, the Mott formula is inapplicable.

A specific feature of thermopower is its sensitivity to the derivative of the reciprocal relaxation time. Therefore, the presence of the θ function in (4) strongly affects the $S(\mu)$ dependence near $|\mu| \approx \Delta$. Here, it is worth mentioning once again that an obvious analogy exists between the transport in gapped graphene and in metals near the topological electron transition. Indeed, near the critical value of the chemical potential $\mu = \mu_c$, where the connectivity of the Fermi surface changes, the relaxation time of quasiparticles becomes substantially energy-dependent, which leads to the appearance of well-known bends in the conductivity curves and of peaks in the thermopower [17].

4. Giant oscillations of the NC in graphene

Giant oscillations of the NC were discovered in 1959 in [25], where this phenomenon was explained as the intersection of the chemical potential by the Landau levels. As in the case of the de Haas–van Alphen oscillations of magnetization and the Shubnikov–de Haas oscillations of conductivity, the fields corresponding to the oscillations of the NC are determined by the Lifshits–Onsager condition [23]

$$S(\mu) = (k + \gamma_\sigma)\, 2\pi\hbar\, \frac{eH_{k\sigma}}{c}\,, \tag{7}$$

where $S(\mu)$ is the area of the Fermi surface cross section corresponding to the orbital motion of electrons at $p_z = 0$, k is an integer, $\gamma_\sigma = \gamma + 1/2\,(m^*/m)\,\sigma$ with $\sigma = \pm 1$, and $m^* = (1/2\pi)\,\mathrm{d}S/\mathrm{d}\mu$ is the cyclotron mass of the electron [23].

Quite recently, the Nernst effect in graphene was studied experimentally [11, 12] and the corresponding results were analyzed in terms of the standard theory [24]. Unexpectedly, it was found that under oscillations, the NC changes sign in graphene in fields that satisfy condition (7), whereas in zinc [25] and bismuth [26], maxima are observed in the corresponding fields. This unusual behavior of the $\nu(H)$ oscillations in graphene is not reproduced in three-dimensional graphite.

One more remarkable property of quantum oscillations is the dependence of their character on the type of the spectrum of charge carriers, namely, on the value of the topological parameter γ [27, 28]: $\gamma = 1/2$ for normal charge carriers (NCCs) with a parabolic two-dimensional (2D) spectrum and Landau linear quantization:

$$\text{NC}: \quad \varepsilon(p_\perp) = \frac{p_\perp^2}{2m_\perp}\,, \quad \varepsilon_k = 2\mu_B H\, \frac{m}{m_\perp}\left(k + \frac{1}{2}\right),$$

and $\gamma = 0$ for Dirac fermions (DFs), which have a linear spectrum with two branches and a square-root dependence of the energy of the Landau levels ($\sim k^{1/2}$) in a magnetic field:

$$\text{DF}: \quad \varepsilon(p_\perp) = \pm v|p_\perp|\,, \quad \varepsilon_k = \pm\left(4mv_\text{F}^2\,\mu_\text{B}\,Hk\right)^{1/2},$$

where $p_\perp$ and $m_\perp$ are the momentum and the effective mass in the plane perpendicular to the magnetic field, m is the mass of a free electron, v_F is its Fermi velocity, and $\mu_\text{B} = e/2mc$ is the Bohr magneton.

Below, we use a simple thermodynamic approach to the description of the Nernst effect, which allows relating the corresponding oscillations with the de Haas–van Alphen oscillations of magnetization. For both contributions to the NC — thermal contribution (Sondheimer [6]) and the contribution corresponding to magnetization currents (Obraztsov [7]) — exact expressions have been found for both parabolic and Dirac spectra. In the last case, our results quite well reproduce the oscillations of the NC found experimentally in graphene [11, 12]. It is remarkable that in contrast to the case of a parabolic spectrum, their amplitude decreases rather than increases with increasing the Fermi energy (voltage at the gate). The shape of the oscillations is determined by the temperature derivative of the de Haas–van Alphen oscillations.

4.1 Thermodynamic description of the Nernst effect

As was mentioned in Section 2, the NC is measured in the absence of currents in the system. Therefore, the electrochemical potential along the temperature gradient can be considered constant, $\mu + e\varphi = \text{const}$ (where φ is the electrostatic potential). Consequently, the effect of temperature inhomogeneity in the sample is determined by the appearance of an effective electric field $E_x = \nabla_x \mu/e$ along the temperature gradient. The problem therefore reduces to the classical Hall problem, which allows easily finding the thermal contribution to the NC,

$$\nu^\text{term} = \frac{\sigma_{xx}}{e^2 nc}\,\frac{\mathrm{d}\mu}{\mathrm{d}T}\,, \tag{8}$$

where n is the concentration of charge carriers. This simple formula reproduces the Sondheimer result for a degenerate electron gas, the fluctuation contribution to the NC in superconductors at temperatures above T_c, etc. [30].

The second contribution to the NC, which arises as a result of the spatial dependence of magnetization in the sample [7], can be found based on the Ampère law. The density of the magnetization current is written as $\mathbf{j}^\text{mag} = [c/(4\pi)]\,\nabla \times \mathbf{B}$, where $\mathbf{B} = \mathbf{H} + 4\pi\mathbf{M}$, $\mathbf{H}$ is the spatially homogeneous magnetic field and $\mathbf{M}$ is the magnetization, which can depend on temperature and, consequently, on the coordinates. The magnetization-related current density is written as $j_y^\text{mag} = -c(\mathrm{d}M/\mathrm{d}T)\,\nabla_x T$; the corresponding contribution to the Nernst electric field is $E_y^\text{mag} = \rho_{yy} j_y^\text{mag}$, where ρ_{yy} is the diagonal component of the resistivity ($\rho_{yy} = \rho_{xx}$). As a result, the contribution from the magnetization currents to the NC is written as

$$\nu^\text{mag} = \frac{c\rho_{yy}}{H}\left(\frac{\mathrm{d}M}{\mathrm{d}T}\right). \tag{9}$$

Relations (8) and (9) allow elucidating the physical nature of oscillations of the NC in quantizing magnetic fields. In particular, they show that the NC depends on the diagonal components of the the conductivity and resistivity tensors, whose oscillations, depending on the magnetic field, are nothing more than the Shubnikov–de Haas effect. However, in graphene, the giant oscillations of the NC are also observed in the state where the Shubnikov–de Has effect is small (at $H < 3$ T) [12]; we should therefore assume that the giant oscillations of the NC in the last case are due to other multipliers that enter into expressions (8) and (9), namely, the temperature derivatives of the chemical potential $\mathrm{d}\mu/\mathrm{d}T$ and magnetization $\mathrm{d}M/\mathrm{d}T$. It is remarkable that to obtain explicit expressions for these quantities, we need no additional information on the transport properties of the system; these derivatives can be expressed in terms of the thermodynamic potential Ω:

$$\frac{\mathrm{d}\mu}{\mathrm{d}T} = \frac{\partial^2\Omega}{\partial T\partial\mu}\left(\frac{\partial^2\Omega}{\partial\mu^2}\right)_T^{-1}, \qquad \frac{\mathrm{d}M}{\mathrm{d}T} = \frac{\partial^2\Omega}{\partial T\partial H}\,. \tag{10}$$

The expression for the oscillating part of the thermodynamic potential in the case of a parabolic spectrum obtained in [31] (see also [32]) was later extended to an arbitrary spectrum $\varepsilon_\perp(p_\perp)$ in [33] (see also [34]). In the 2D case, we have

$$\widetilde{\Omega} = \frac{m^*}{2\pi\hbar^2}\,\frac{\hbar^2\omega_\text{c}^2}{\pi^2}\,\frac{1}{2}\sum_{l=1,\,\sigma=\pm1}^{\infty}\frac{\psi(\lambda l)}{l^2}\exp\left(-\frac{2\pi l\Gamma}{\hbar\omega_\text{c}}\right) \times\cos\left[2\pi l\left(\frac{c}{e\hbar}\,\frac{S(\mu)}{2\pi H} - \gamma_\sigma\right)\right], \tag{11}$$

with $\psi(\lambda l) = \lambda l/\sinh\lambda l$. Here, $\lambda = 2\pi^2 T/(\hbar\omega_\text{c})$ and Γ is the Dingle broadening of the Landau level. To apply the results to both the parabolic and Dirac spectra, we represent expression (11) in the most general form using the parameters S, m^*, ω_c, and γ_σ. In the case of NCCs, we have $S = 2\pi m_\perp\,\mu$, $m^* = m_\perp$, $\omega_\text{c} = eH/m_{\perp\text{c}}$, and $\gamma_\sigma = 1/2 + (1/2)\,(m_\perp/m)\,\sigma$; in the case of DFs, $S = \pi\mu^2/v^2$, $m^* = \mu/v^2$, $\omega_\text{c} = eHv^2/(\mu c)$, and $\gamma_\sigma = 1/2\,[\mu/(mv^2)]\,\sigma$. As a result, the oscillating parts of the magnetization and chemical potential can be expressed, using relation (10), in the form

$$\frac{\mathrm{d}\widetilde{\mu}}{\mathrm{d}T} = -\frac{\operatorname{Im}\Xi^{\{1\}}}{1 + 2\operatorname{Re}\Xi^{\{0\}}}\,, \quad \frac{\mathrm{d}\widetilde{M}}{\mathrm{d}T} = \frac{n}{H}\,\frac{\mathrm{d}\widetilde{\mu}}{\mathrm{d}T}\,, \tag{12}$$

where

$$\Xi^{\{\alpha\}} = \frac{1}{2}\sum_{l=1,\,\sigma=\pm1}^{\infty}\psi^{(\alpha)}(\lambda l)\exp\left(-\frac{2\pi l\Gamma}{\hbar\omega_\text{c}}\right) \times\cos\left[2\pi l\left(\frac{c}{e\hbar}\,\frac{S(\mu)}{2\pi H} - \gamma_\sigma\right)\right], \tag{13}$$

and $\psi^{(\alpha)}(x)$ is the derivative of ψ of the order $\alpha = 0, 1$. It follows from (9) and (12) that the NC oscillates proportionally to the temperature derivative of the magnetization. This fact suggests the existence of an important universal (independent of the dimensionality and type of charge carriers) relation between the oscillations of the NC and the de Haas–van Alphen effect.

It is convenient to represent the NC in the form

$$\nu = \nu^\text{term} + \nu^\text{mag} = \nu_0(H) + \widetilde{\nu}(H)\,, \tag{14}$$

where $\nu_0(H)$ and $\widetilde{\nu}(H)$ are respectively the background and oscillating parts. The background part can be found in the Drude-theory approximation [30]:

$$\nu_0(H) = \frac{\pi^2\tau}{6m^*c}\left(\frac{T}{\varepsilon_\text{F}}\right)\frac{1}{1 + (\omega_\text{c}\tau)^2}\,. \tag{15}$$

Taking the magnetization currents into account here leads to the appearance of a correction to the Sondheimer's result (15) of the order $(\varepsilon_F\tau)^{-2}$.

Using (8), (9), and (12), the oscillating part of the NC can be represented as

$$\tilde{\nu}(H) = -2\pi\kappa(H)\frac{\operatorname{Im}\Xi^{\{1\}}}{1+2\operatorname{Re}\Xi^{\{0\}}}, \tag{16}$$

where

$$\kappa(H) = \frac{\sigma_{xx}(H)}{e^2nc} + \frac{cn\rho_{xx}(H)}{H^2}. \tag{17}$$

Expression (16) describes the oscillations of the NC in the most general form, which is valid for an arbitrary type of the spectrum of charge carriers $\varepsilon_\perp(p_\perp)$.

4.2 Shape of oscillations and its dependence on the type of carriers

We analyze expression (16) in the limit of low temperatures, $2\pi^2T < \hbar\omega_c$. In this case, the parameter λ in (11) is much less than unity; consequently, $\psi(\lambda l) \approx 1-(1/6)\lambda^2l^2$. For $m^* < 0.02m$ and $H = 10$ T (typical values in experiments on graphene), this requirement means that $T < 10$ K. Because $m^* \ll m$, we can neglect the Zeeman splitting, assuming that $\gamma_\sigma = 0$ for the NCCs and $\gamma_\sigma = 1/2$ for the DFs. The series $\Xi^{\{0\}}$ and $\Xi^{\{1\}}$ in (16) in this case can be summed analytically:

$$\tilde{\nu}^{(2D)}(\mu,H) = \frac{2\pi^3}{3}\frac{T}{\hbar\omega_c}\kappa(H) \times \frac{\sin 2\pi\{[c/(e\hbar)]\,[S(\mu)/(2\pi H)]-\gamma\}}{\cosh[2\pi\Gamma/(\hbar\omega_c)]-\cos 2\pi\{[c/(e\hbar)][S(\mu)/(2\pi H)]-\gamma\}}. \tag{18}$$

In experiments involving measurements of the NC in graphene, the number of particles is usually fixed; therefore, we have the relation [31]

$$n = -\left(\frac{\partial\Omega(\mu)}{\partial\mu}\right)_{H,T} = 2\frac{S(\mu)}{(2\pi\hbar)^2} - \left(\frac{\partial\tilde{\Omega}(\mu)}{\partial\mu}\right)_{H,T} = \text{const} \tag{19}$$

(we assume that the volume is $V = 1$). This equation implicitly determines the dependence of the chemical potential μ on H and T at a given n. We note that according to (19), the chemical potential μ is a function of the magnetic field H. The corresponding expression for $S(\mu)$ is

$$\frac{c}{e\hbar}\frac{S(\mu)}{2H} = \pi^2\frac{\hbar c}{e}\frac{n}{H} - \arctan\frac{\sin 2\pi[\pi(\hbar c/e)\,n/H-\gamma]}{\exp(2\pi\Gamma/\hbar\omega_c)+\cos 2\pi[\pi(\hbar c/e)\,n/H-\gamma]}. \tag{20}$$

Relation (20) gives the sought dependence $\mu(n,H)$. Substituting (20) in (18), after laborious calculations, we can find the oscillating part of the NC in the explicit form

$$\tilde{\nu}^{(2D)}(n,H) = \frac{2\pi^3}{3}\frac{T}{\hbar\omega_c}\frac{\kappa(H)}{\sinh(2\pi\Gamma/\hbar\omega_c)} \times \sin 2\pi\left(\pi\frac{\hbar c}{e}\frac{n}{H}-\gamma\right). \tag{21}$$

We see that Eqn (21) is a strongly oscillating function that vanishes in magnetic fields in which Landau levels cross the chemical potential ($H = H_{k\sigma}$ is determined by condition (7)). The magnetic-field-dependent factor $\kappa(H)$, which is determined by the behavior of the magnetoresistance, is given by (17). At $\omega_c\tau \leqslant 1$, when the Shubnikov–de Haas oscillations are small, $\kappa(H)$ can be estimated in the Drude approximation. In particular, in the limit where $\omega_c\tau \sim 1$, we obtain (assuming that $\Gamma \sim \hbar/2\tau$) $\kappa(H) \sim \tau/(m^*c)$, and the amplitude of NC oscillations turns out to be giant compared to the background magnitude $\tilde{\nu}^{(2D)} \sim [\varepsilon_F/(\hbar\omega_c)]\,\nu_0$. In stronger fields ($\omega_c\tau > 1$), under the quantum Hall effect, the shape of NC oscillations begins to be determined by the sharp dependence of the magnetoconductivity and of the Dingle temperature on the magnetic field. This circumstance can be taken into account by the substituting the appropriate dependences in Eqns (16) and (17).

Figure 2a displays the oscillations of the NC as a function of the inverse magnetic field for the two-dimensional system with parabolic and Dirac spectra in accordance with Eqn (21). Both theoretical and experimental results obtained for graphene [11, 12] exhibit a sinusoidal profile of the signal,

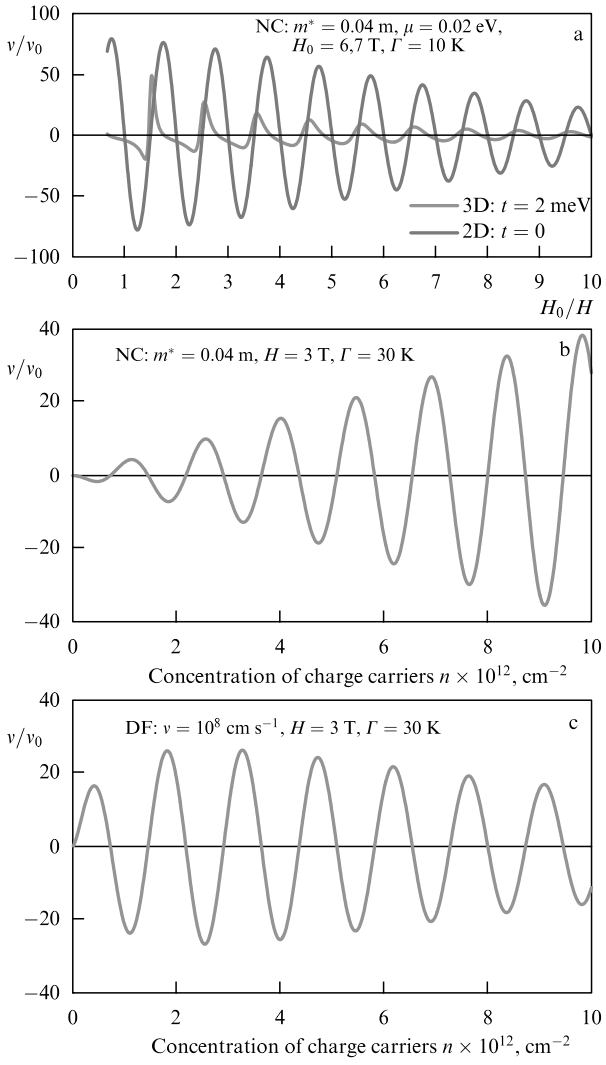

Figure 2. (a) Oscillations of the NC as a function of the inverse magnetic field and the concentrations of charge carriers (b) with a parabolic spectrum (NCC) and (c) for Dirac fermions (DF). The $\nu(H^{-1})$ dependence for the DFs has the same shape as the dependence for the NCCs, but is shifted relative to the latter by a half-period. The vertical straight lines indicate the field values at which quantization condition (7) is satisfied.

whose amplitude decreases slowly with increasing the concentration of charge carriers with the Dirac spectrum. This behavior contradicts the theoretical predictions based on the classical Mott formula applied to the Boltzmann electron gas [11]. On the contrary, in the case of charge carriers with a parabolic spectrum, our theory predicts an increase in the amplitude of oscillations with increasing the concentration of charge carriers. The last statement agrees qualitatively with the results obtained using the Mott formula.

Acknowledgments. This work was supported in part by the SIMTECH project (New Century of Superconductivity: Ideas, Materials and Technologies) No. 246937 within the European program FP7.

References

1. Geim K L *Science* **324** 1530 (2009)
2. Grosse K L et al. *Nature Nanotechnol.* **6** 287 (2011)
3. Mott N F, Jones H *The Theory of the Properties of Metals and Alloys* 1st ed. (Oxford: Clarendon Press, 1936)
4. Von Ettingshausen A, Nernst W *Ann. Physik* **265** 343 (1886)
5. Behnia K, Méasson M-A, Kopelevich Y *Phys. Rev. Lett.* **98** 076603 (2007)
6. Sondheimer E H *Proc. R. Soc. London A* **193** 484 (1948)
7. Obraztsov Yu N *Fiz. Tverd. Tela* **6** 414 (1964) [*Sov. Phys. Solid State* **6** 331 (1964)]
8. Sharapov S G, Varlamov A A *Phys. Rev. B* **86** 035430 (2012)
9. Luk'yanchuk I A, Varlamov A A, Kavokin A V *Phys. Rev. Lett.* **107** 016601 (2011)
10. Wei P et al. *Phys. Rev. Lett.* **102** 166808 (2009)
11. Zuev Y M, Chang W, Kim P *Phys. Rev. Lett.* **102** 096807 (2009)
12. Checkelsky J G, Ong N P *Phys. Rev. B* **80** 081413(R) (2009)
13. Wang D, Shi J *Phys. Rev. B* **83** 113403 (2011)
14. Löfwander T, Fogelström M *Phys. Rev. B* **76** 193401 (2007)
15. Hwang E H, Rossi E, Das Sarma S *Phys. Rev. B* **80** 235415 (2009)
16. Ugarte V, Aji V, Varma C M *Phys. Rev. B* **84** 165429 (2011)
17. Varlamov A A, Egorov V S, Pantsulaya A V *Adv. Phys.* **38** 469 (1989)
18. Zhou S Y et al. *Nature Mater.* **6** 770 (2007)
19. Li G, Luican A, Andrei E Y *Phys. Rev. Lett.* **102** 176804 (2009)
20. Peres N M R, Lopes dos Santos J M B, Stauber T *Phys. Rev. B* **76** 073412 (2007)
21. Gorbar E V et al. *Phys. Rev. B* **66** 045108 (2002)
22. Gusynin V P, Sharapov S G *Phys. Rev. B* **71** 125124 (2005); *Phys. Rev. B* **73** 245411 (2006)
23. Lifshits I M, Kosevich A M *Zh. Eksp. Teor. Fiz.* **29** 730 (1955) [*Sov. Phys. JETP* **2** 636 (1956)]
24. Bergman D L, Oganesyan V *Phys. Rev. Lett.* **104** 066601 (2010)
25. Bergeron C J, Grenier C G, Reynolds J M *Phys. Rev. Lett.* **2** 40 (1959)
26. Behnia K, Méasson M-A, Kopelevich Y *Phys. Rev. Lett.* **98** 166602 (2007)
27. Falkovsky L A *Zh. Eksp. Teor. Fiz.* **49** 609 (1965) [*Sov. Phys. JETP* **22** 423 (1966)]
28. Mikitik G P, Sharlai Yu V *Phys. Rev. Lett.* **82** 2147 (1999)
29. Serbyn M N et al. *Phys. Rev. Lett.* **102** 067001 (2009)
30. Varlamov A A, Kavokin A V *Europhys. Lett.* **86** 47007 (2009)
31. Champel T, Mineev V P *Phylos. Mag. B* **81** 55 (2001)
32. Bratkovsky A M, Alexandrov A S *Phys. Rev. B* **65** 035418 (2002)
33. Luk'yanchuk I A, Kopelevich Y *Phys. Rev. Lett.* **93** 166402 (2004)
34. Sharapov S G, Gusynin V P, Beck H *Phys. Rev. B* **69** 075104 (2004)